Long Noncoding RNA ZFPM2-AS1 Knockdown Restrains the Development of Retinoblastoma by Modulating the MicroRNA-515/HOXA1/Wnt/β-Catenin Axis

Xueman Lyv,[1,2] Fei Wu,[3] Hong Zhang,[1] Jia Lu,[1] Lina Wang,[1] and Yunhai Ma[2]

[1]Department of Ophthalmology, China-Japan Union Hospital of Jilin University, Changchun, Jinlin, People's Republic of China
[2]Key Laboratory of Bionic Engineering (Ministry of Education), Jilin University (Nanling Campus), Changchun, Jinlin, People's Republic of China
[3]Department of Gynecology and Obstetrics, The Second Hospital of Jilin University, Changchun Jinlin, People's Republic of China

Correspondence: Lina Wang, Department of Ophthalmology, China-Japan Union Hospital of Jilin University, No. 126, Xiantai Street, Changchun 130031, Jilin, People's Republic of China; Wanglina12131@163.com.
Yunhai Ma, Key Laboratory of Bionic Engineering (Ministry of Education), Jilin University (Nanling Campus), No. 5988, Renmin Street, Changchun 130022, Jilin, People's Republic of China; yanmao6123375@163.com.

Received: February 7, 2020
Accepted: May 20, 2020
Published: June 19, 2020

Citation: Lyv X, Wu F, Zhang H, Lu J, Wang L, Ma Y. Long noncoding RNA ZFPM2-AS1 knockdown restrains the development of retinoblastoma by modulating the microRNA-515/HOXA1/Wnt/β-catenin axis. *Invest Ophthalmol Vis Sci.* 2020;61(6):41. https://doi.org/10.1167/iovs.61.6.41

Purpose. The tumor-initiating function of long non-coding RNA (lncRNA), zinc finger protein multitype 2 antisense RNA 1 (ZFPM2-AS1) was reported in lung cancer, yet the relevance of ZFPM2-AS1 in retinoblastoma (RB), a malignancy representing 2.5% to 4% incidence of cancers among children, has not been elucidated. Thus, we attempted to assess the effect of ZFPM2-AS1 and underlying mechanism in RB progression.

Methods. First, comparing the differentially expressed lncRNAs in normal retinal tissues as well as RB tissues, the target lncRNA ZFPM2-AS1 was screened out. We then assayed the ZFPM2-AS1 expression in three RB cell lines, and carried out methylthiazol tetrazolium (MTT), transwell assays, and flow cytometric analyses to examine the role of si-ZFPM2-AS1 on cell behaviors. Following online database predication, the correlations between ZFPM2-AS1 and microR-515 (miR-515) or homeobox A1 (HOXA1) were corroborated by dual-luciferase reporter gene assays. Quantitative real-time PCR along with Western blot assays was fulfilled to ascertain the expression of relevant genes.

Results. ZFPM2-AS1 was significantly overexpressed in RB tissues and cell lines, and ZFPM2-AS1 silencing curtailed the growth and metastasis of RB cells both in vitro and in vivo. Bioinformatic websites and dual-luciferase reporter gene assays disclosed that ZFPM2-AS1 might perform as a competing endogenous RNA for miR-515 and positively correlate with HOXA1 to activate the Wnt/β-catenin signaling pathway.

Conclusions. Altogether, these data demonstrated that ZFPM2-AS1 interacted with HOXA1 to promote RB development via mediating miR-515, establishing a promising therapeutic biomarker for RB and prognosis.

Keywords: retinoblastoma, long non-coding RNA ZFPM2-AS1, microRNA-515, HOXA1, Wnt/β-catenin pathway, metastasis

Retinoblastoma (RB), either in a sporadic or a heritable form, is an infrequent childhood cancer of the retina and may be lethal if untreated.[1] The last decade saw major changes in conventional treatments for intraocular RB, and combinations of ophthalmic artery chemosurgery and intravitreous chemotherapy are now the standard treatments for the majority of unilateral RB and certain bilateral cases.[2] RB could metastasize to the regional lymph nodes, the central nervous system, as well as distant organs.[3] Once metastasis occurred, the survival rate of patients with RB was profoundly deteriorated, therefore, understanding the mechanisms and developing new therapeutic treatments for RB has become an urgency.[4]

Long noncoding RNAs (lncRNAs) that are > 200 nt long play crucial parts in modulating gene expression, cell growth, and differentiation, as well as development.[5] A plethora of common lncRNAs, such as HOX antisense intergenic RNA[6] and X inactive specific transcript,[7] were monitored as oncogenes in RB by stimulating cell migration and invasion events or enhancing epithelial to mesenchymal transition (EMT). Interestingly, zinc finger protein multitype 2 antisense RNA 1 (ZFPM2-AS1) has been previously linked to clinical aggressiveness and low survival of patients with gastric carcinogenesis.[8] Moreover, ZFPM2-AS1 depletion hampered lung adenocarcinoma cell proliferation, migration, and reversed the progress of EMT.[9] Besides, microR-515 (miR-515)-5p was disclosed to inhibit the cell survival and metastasis in non-small cell lung cancer,[10] indicating a possible correlation between ZFPM2-AS1 and miR-515 in cancers. In this study, homeobox transcription factor A1 (HOXA1) is validated to bind to and is negatively regulated by miR-515. HOXA1, belonging to the

Table 1. Clinical Baseline Information of 51 Patients With RB

Parameters		Cases (n = 51)
Age, y	< 3	32 (62.74%)
	≧ 3	19 (37.26%)
Sex	Male	25 (49.02%)
	Female	26 (50.98%)
IIRC stage	Early stage	18 (35.29%)
	Advanced stage	33 (64.71%)
Optic nerve invasion	Negative	27 (52.94%)
	Positive	24 (47.06%)
Differentiation grade	Well/moderately differentiated	30 (58.82%)
	Poorly differentiated	21 (41.18%)

RB, retinoblastoma; IIRC, intraocular international retinoblastoma classify.

homeobox transcription factor family, which is made up of 39 human genes, demonstrates pro-invasion and oncogene potencies in several melanoma cells.[11] In addition, HOXA1 knockdown was reported to repress growth and metastasis in prostate cancer.[12] In another research regarding RB, HOXB5 facilitated the cell migration and invasion by inducing the ERK1/2 pathway.[13] The positive correlation between HOXA1 expression and the activation of Wingless and Int1 (Wnt)/β-catenin pathway was confirmed in breast cancer in a former study,[14] which is regarded as a vital communication pathway that mediates proliferation and differentiation of cells in the retina tissues.[15] The main purposes of our investigation were to study the effects of ZFPM2-AS1 and miR-515 on RB cell proliferation, migration, and invasion, as well as the correlation between ZFPM2-AS1 and miR-515. In addition, the potential downstream molecule HOXA1 and possible signaling pathway Wnt/β-catenin were also analyzed. These results will be beneficial for further comprehension the RB pathogenesis and for offering possible targets for RB treatment.

Materials and Methods

Ethics Approval and Consent to Participate

Written informed consent was attained from patient's legal guardians. The collection and application of clinical samples were under the approval of the independent review board of China-Japan Union Hospital of Jilin University. All experiments involving animals were performed strictly following the recommendations from the Guide for the Care and Use of Laboratory Animals of the National Institutes of Health.

Patient Population

A total of 51 human RB tissues collected from 33 boys and 18 girls ranging in age from 6 months to 16.6 years with an average age of 5.2 years and 17 normal retinal tissues from 9 boys and 8 girls ranging in age from 4.4 to 14.8 years with an average age of 6.9 years were enrolled in this study. Because the majority of patients were infants, radiotherapy and chemotherapy were not applicable, and surgical removal was performed as the primary treatment. RB samples were collected during enucleation surgery. Normal retinal tissues were harvested from donors who died from causes other than RB. No patient received pre-operative treatment. RB tissues and normal retinal tissues were rapidly frozen in liquid nitrogen and subsequently preserved at −80 deg Celsius (°C). The histological and pathological diagnosis of these samples were substantiated and categorized by two experienced clinical pathologists. Detailed clinical baseline information for 51 patients is listed in Table 1.

Microarray Analysis

We performed lncRNA microarray analysis on tumor tissues from six patients with RB and three normal retinal tissues using Arraystar Human LncRNA Microarray version 5.0 technology (Agilent Technologies, Santa Clara, CA, USA). Initially, we used TRIzol reagents to extract the total RNA from the tissues, and then NanoDrop 2000 was used to determine the purity and quantity of the RNA. cDNA was synthesized and labeled with biotin. The labeled probes were hybridized with high density microarrays under standard conditions. After hybridization, the fluorescence intensity of the microarray was scanned with a GenePix-4000B scanner, and the results were converted to digital for preservation. The raw data were analyzed using Agilent feature extraction software to analyze. Significantly differential lncRNAs with foldchange > 2.0 and $p < 0.05$ were used and were screened out.

Cell Lines and Transfection

Human RB cells WERI-RB1, SO-RB50, and Y79, as well as human retinal pigment epithelial cells ARPE-19 were from American Type Culture Collection (Manassas, VA, USA) and kept at 37°C in Roswell Park Memorial Institute (RPMI)-1640 medium (Gibco, Carlsbad, CA, USA) with the addition of 10% fetal bovine serum (FBS; Hyclone, Marlborough, MA, USA) with 5% CO_2. ZFPM2-AS1 specific short hairpin RNAs (shRNAs; sh-ZFPM2-AS1-1# and sh-ZFPM2-AS1-2#), shRNA-negative control (Scramble), ZFPM2-AS1 expression vector, empty vector, miR-515 mimic, mimic control (Mock), HOXA1 expression vector, and empty vector were all synthesized by GenePharma (GenePharma, Shanghai, China). The transfection procedure was conducted using Lipofectamine2000 reagent (Invitrogen). Simply put, cells were seeded in 6-well plates at a density of 2×10^5 cells each well and transfected using Lipofectamine 2000 in Opti-MEM I Reduced Serum Medium (Gibco) with 125 pmoL shRNAs. At 48 hours post-transfection, cells were collected in TRIzol for RNA separation or lysed in radio immunoprecipitation assay buffer (RIPA) lysis buffer for Western blot.

Investigative Ophthalmology & Visual Science

Table 2. Primers Used in This Study

Targets	Forward (5'-3')	Reverse (5'-3')
ZFPM2-AS1	GTGACTTGGCAAGGAGTGGAAG	CATCTGACTGGCAGCTTGTAGC
E-cadherin	GCCTCCTGAAAAGAGAGTGGAAG	TGGCAGTGTCTCTCCAAATCCG
N-cadherin	CCTCCAGAGTTTACTGCCATGAC	GTAGGATCTCCGCCACTGATTC
miR-515	TTCTCCAAAAGAAAGCACT	GAACATGTCTGCGTATCTC
HOXA1	CAGCGCAGACTTTTGACTGGATG	TCCTTCTCCAGTTCCGTGAGCT
U6	CTCGCTTCGGCAGCACAT	TTTGCGTGTCATCCTTGCG
GAPDH	GTCTCCTCTGACTTCAACAGCG	ACCACCCTGTTGCTGTAGCCAA

ZFPM2-AS1, zinc finger protein multitype 2 antisense RNA 1; miR-515, microRNA-515; HOXA1, homeobox A1; GAPDH, glyceraldehyde 3-phosphate dehydrogenase.

Reverse Transcription Quantitative Polymerase Chain Reaction

Total RNA in tissue samples and cells was harvested using Trizol reagent (Takara Holdings Inc., Kyoto, Japan). Taqman Advanced miRNA cDNA Synthesis Kit (Thermo Fisher Scientific Inc., Waltham, MA, USA) and Reverse Transcript Kit (Applied Biosystems, Inc., Foster City, CA, USA) were then utilized for reverse transcription. Subsequently, the expression of ZFPM2-AS1 was detected by SYBR Green quantitative PCR Mix (Thermo Fisher Scientific Inc., Waltham, MA, USA) kit with ABI real-time fluorescence quantitative PCR platform (Thermo Fisher). Glyceraldehyde 3-phosphate dehydrogenase (GAPDH) and U6 were utilized as housekeeping genes. Details of primers are listed in Table 2.

Cell Activity Measurement

A 3-(4,5-Dimethylthiazol-2-Yl)-2,5-Diphenyltetrazolium Bromide (MTT) kit (Beyotime Biotechnology Co., Ltd., Shanghai, China) was applied to evaluate the proliferation activity of Y79 and WERI-RB1 cells. In short, cells were seeded in 96-well plates and added with 10 µL MTT solution at the first, second, and third day of culture. The optical density (OD) values at 570 nm were recorded.

Next, apoptosis was assessed using the Annexin V-fluorescein isothiocyanate (FITC)/propidium iodide (PI) apoptosis detection kit (NanJing Vazyme Biotech Co., Ltd., Nanjing, China) according to the manufacturer's protocol. The cells were analyzed by a flow cytometer using BD FACSCanto II (BD Biosciences, San Jose, CA, USA) and by FlowJo software (Tree Star Software, San Carlos, CA, USA).

At length, RB cell migration and invasion capabilities were tested as described previously.[16] In brief, cell migration and invasion tests were measured by Transwell chambers (8 µM; BD Biosciences). For invasion assay, cells were added to the apical chamber coated with 50 µL Matrigel (BD Biosciences) and cultured in serum-free medium. The basolateral chamber was loaded with RPMI-1640 medium containing 20% FBS. For migration assay, no Matrigel was used. After 24 hours of culture, the invaded or migrated cells were fixed, stained with 1% crystal violet, and counted for examination under a microscope (Olympus, Tokyo, Japan).

Detection of Epithelial-Mesenchymal Transition Markers

Afterward, we used immunofluorescence to evaluate the expression patterns of epithelial marker E-cadherin and interstitial marker N-cadherin in Y79 and WERI-RB1 cells, as previously reported.[17] Cells were seeded on slides in each well, fixed with 4% paraformaldehyde at room temperature for 15 minutes, and then permeated in phosphate buffered saline (PBS) with 0.5% Triton X-100. After a 1-hour sealing in 1% gelatin in the PBS, the cells were incubated with rabbit monoclonal antibodies against E-cadherin (AlexaFluor488 conjugated, Cell Signaling Technologies (CST), Beverly, MA, USA; #3199; 1:200) or N-cadherin (AlexaFluor488 conjugated, Cell Signaling Technologies (CST), #81673; 1:800) overnight at 4°C. Then the cells were incubated with 5 µg/mL 4',6-diamidino-2-phenylindole (Sigma-Aldrich Chemical Company, St Louis, MO, USA) at room temperature for 30 minutes and observed under an LSM 5Pa laser scanning microscopy (Carl Zeiss, Oberkochen, Germany).

Nuclear-Cytoplasmic Fractionation

First, we used Lncatlas (http://lncatlas.crg.eu/) to predict the subcellular localization of ZFPM2-AS1. A PARIS kit (AM1921; Invitrogen; Thermo Fisher Scientific, Inc.) was used to separate nuclear and cytosolic fractions of Y79 and WERI-RB1 cells according to protocols provided by the manufacturer.

Fluorescence In Situ Hybridization

Cy3 labeled ZFPM2-AS1 probes were designed and synthesized by Takara Holdings Inc. (Kyoto, Japan). The length of the probe is about 27 nucleotides. ZFPM2-AS1 were hybridized in situ with Cy3 labeled ZFPM2-AS1 probes in Y79 and WERI-1 cells according to the manufacturer's protocol of the FISH kit (Guangzhou RiboBio Co., Ltd., Guangzhou, Guangdong, China). Y79 and WERI-1 were fixed in 4% paraformaldehyde at room temperature for 10 minutes and incubated in PBS containing 0.5% Triton X-100 at 4°C for 5 minutes. To perform pre-hybridization, Y79 and WERI-1 were incubated in pre-hybridization buffer at 37°C for 30 minutes. The subcellular localization of ZFPM2-AS1-202 was detected by a laser scanning confocal microscope (Carl Zeiss AG).

Luciferase Reporter Assay

The binding relationship of miR-515 to ZFPM2-AS1 and HOXA1 was determined by luciferase reporter tests. Synthesis of ZFPM2-AS1 or HOXA1 wild-type (WT) and 3′untranslated region (3′UTR) binding sequence mutant (MT) was commissioned to GenePharma Bioengineering Co., Ltd. (Shanghai, China) and insertion into pMIR-REPORT (Thermo Fisher Scientific). Luciferase activity intensity was then assessed by a dual-luciferase reporter assay system (Promega).

Investigative Ophthalmology & Visual Science

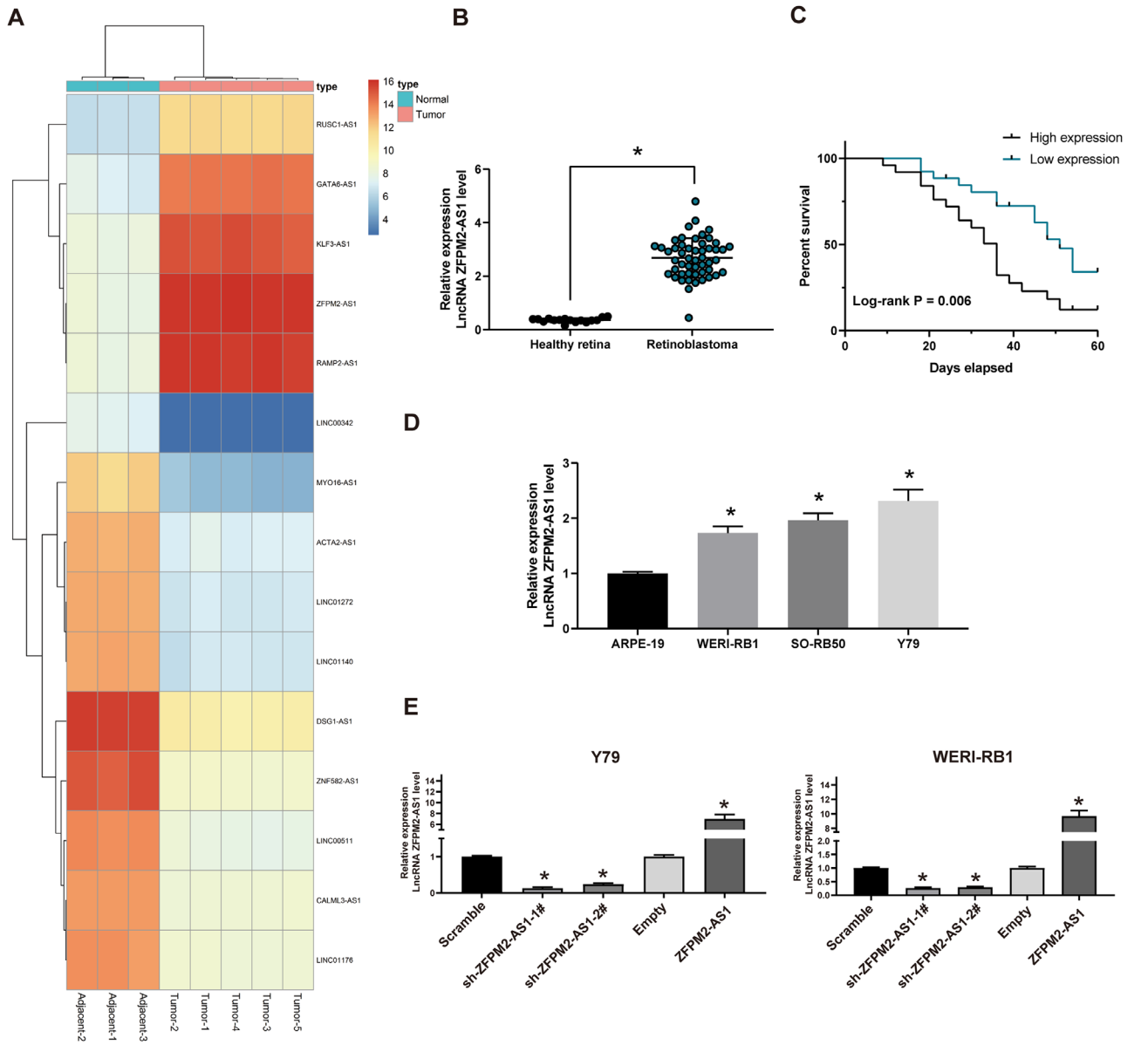

Figure 1. High ectopic expression of ZFPM2-AS1 is identified in RB tissue. (**A**) The heatmap for 15 ectopic expressed lncRNAs in RB. (**B**) ZFPM2-AS1 expression in RB tissue compared with healthy retina tissues determined by RT-quantitative PCR. (**C**) Kaplan–Meier survival analysis demonstrating the overall survival of patients with relatively high or low ZFPM2-AS1. (**D**) RT-quantitative PCR analysis of ZFPM2-AS1 expression in RB cells and the ARPE-19 cells. (**E**) RT-quantitative PCR analysis of ZFPM2-AS1 expression pattern in Y79 and WERI-RB1 cells after different transfection. The data are expressed as the mean ± SD. One-way ANOVA and Tukey's multiple comparison test was used to determine statistical significance, $^*P < 0.05$.

Enzyme Linked Immunosorbent Assay

ELISA kits (Abcam Inc., Cambridge, UK) was applied to determine the expression of Wnt1 and β-catenin in the Wnt/β-catenin signaling pathway following the instructions.

Western Blot

The cells were lysed using RIPA. The same amount of protein samples was loaded onto 10% sodium dodecyl sulfate polyacrylamide gels and transferred to the polyvinylidene difluoride membrane (Millipore Corp., Billerica, MA, USA). The membranes were incubated overnight with antibodies against Wnt1 (ab15251), β-catenin (ab32572), and GAPDH (all 1:1000, ab181607; Abcam) at 4°C, respectively. Then, the membrane was incubated with the secondary antibody at room temperature for 2 hours. The protein bands were visualized by chemiluminescence. GAPDH antibody was used as loading control.

In Vivo Experiments

BALB/c nude mice (4–6 weeks old; Shanghai Lab Animal Research Center, Shanghai, China) were raised in specific-pathogen-free facilities. A total of 1×10^6 Y79 cells transfected with siRNA-ZFPM2-AS1 was delivered into the left and right armpit of the mice for tumorigenicity observation. A total of 1×10^6 cells was administrated via caudal

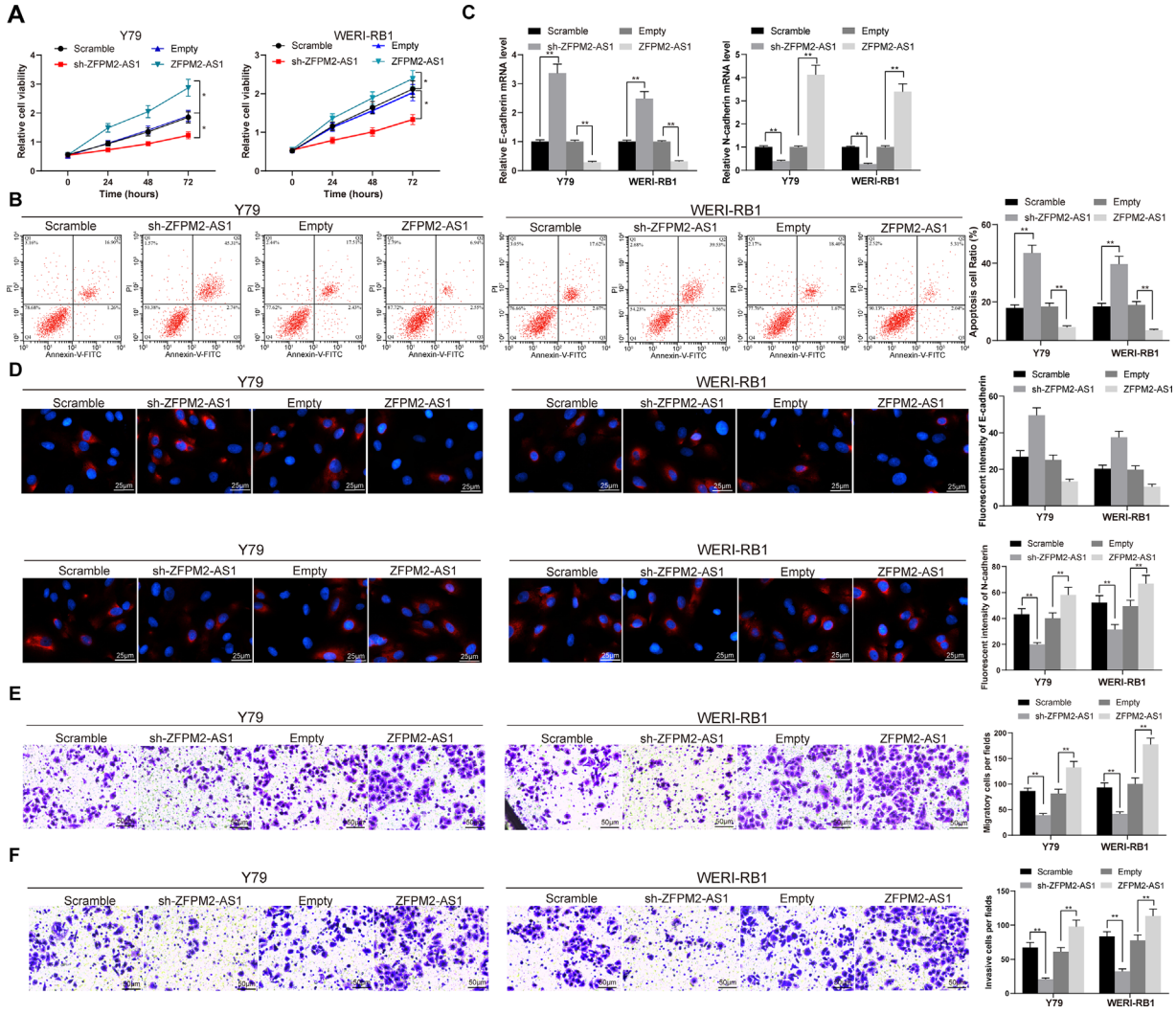

Figure 2. ZFPM2-AS1 knockdown inhibits RB cell viability. (**A**) Y79 and WERI-RB1 cell viability determined by MTT assays. (**B**) PI/Annexin-V-stained Y79 and WERI-RB1 cells determined by flow cytometry. (**C**) E-cadherin and N-cadherin mRNA expression determined by RT-quantitative PCR. (**D**) E-cadherin and N-cadherin expression determined by immunofluorescence. (**E**) Y79 and WERI-RB1 cell migration determined by transwell assays. (**F**) Y79 and WERI-RB1 cell invasion determined by transwell assays. The data are expressed as the mean ± SD. One-way ANOVA and Tukey's multiple comparison test was used to determine statistical significance, $^{*}P < 0.05$, $^{**}P < 0.01$.

vein for lung metastasis and liver metastasis determination. Tumor volume was measured regularly. The tumor weight was finally measured in mice after being euthanized (overdose of pentobarbital sodium at 100 mg/kg). The whole lung and liver tissues were removed and fixed with fixative diluted with neutral buffered formalin at 1:5 to observe the metastatic nodules. The excised tumors and lungs were fixed and paraffin-embedded for staining detection.

Statistical Analysis

Statistical analysis was conducted applying SPSS version 21.0 software (IBM Corp., Armonk, NY, USA). Data were displayed as mean ± SD after Kolmogorov-Smirnov test for normal distribution. The one-way or two-way analysis of variance (ANOVA) following Tukey's post hoc test were performed to exhibit the differences among experimental groups. When p value was < 0.05, the results were thought to be statistically significant.

Results

ZFPM2-AS1 Overexpressed in RB is Associated With Dismal Prognosis

We first analyzed the differentially expressed lncRNAs in tumor tissues from six patients with RB and three normal retinal tissues by microarray analysis. The top 10 lncRNAs with the most significant expression were shown in the heatmap (Fig. 1A). Subsequently, we demonstrated by further experiments that ZFPM2-AS1 expression in tissues from 51 patients with RB was remarkably elevated versus that in 17 normal retinal tissues (Fig. 1B). Moreover, Kaplan–Meier analysis as well as log rank test revealed a close correlation between overexpression of ZFPM2-AS1 and a worse prognosis in RB (Fig. 1C). Correspondingly, ZFPM2-AS1 expression in the RB cells was markedly promoted in comparison with the normal retinal cells (Fig. 1D). To further determine the biological function of ZFPM2-AS1 in RB growth and metastasis, Y79 and WERI-RB1 cells were trans-

Investigative Ophthalmology & Visual Science

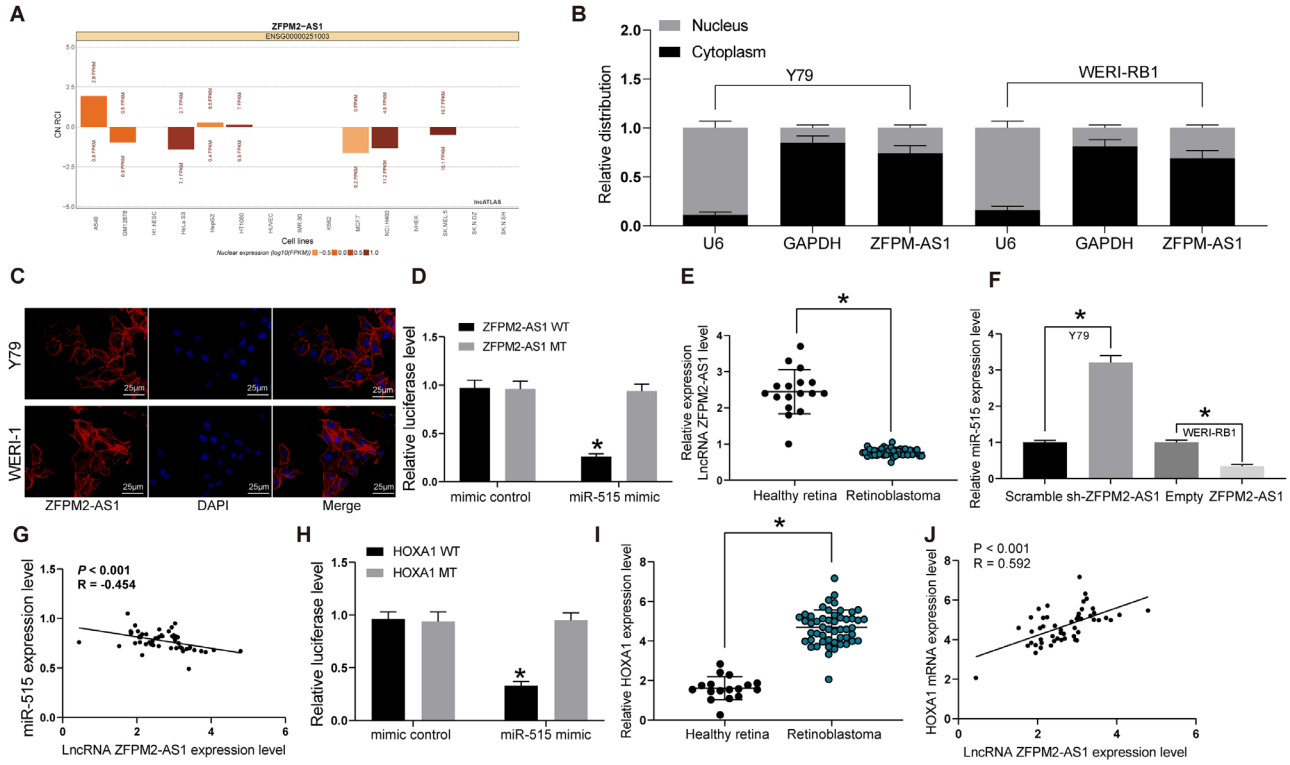

Figure 3. ZFPM2-AS1 enhances HOXA1 expression by sponging miR-515. (**A**) LncAtlas predicted LncRNA ZFPM2-AS1 subcellular location. (**B**) Nuclear and cytoplasmic expression of ZFPM2-AS1 in Y79 and WERI-RB1 cells determined by RT-quantitative PCR. (**C**) ZFPM2-AS1 subcellular localization in Y79 and WERI-1 cells detected by FISH. (**D**) ZFPM2-AS1 and miR-515 combination evaluated by dual luciferase assays. (**E**) MiR-515 expression in RB tissues and healthy retina tissues evaluated by RT-quantitative PCR. (**F**) MiR-515 expression determined in Y79 and WERI-RB1 cells. (**G**) Pearson's correlation scatter plot of ZFPM2-AS1 expression and miR-515 expression in RB samples. (**H**) HOXA1 and miR-515 combination examined by dual luciferase assays. (**I**) HOXA1 expression in RB tissues compared with healthy retina tissues determined by RT-quantitative PCR. (**J**) Pearson's correlation scatter plot of ZFPM2-AS1 expression and HOXA1 expression in RB tissues. The data are expressed as the mean ± SD. One-way ANOVA and Tukey's multiple comparison test was used to determine statistical significance, $^*P < 0.05$.

fected with pcDNA3.1 ZFPM2-AS1 and ZFPM2-AS1 shRNA. RT-quantitative PCR validated the successful deliveries into these two RB cell lines (Fig. 1E). Altogether, these findings specified that ZFPM2-AS1 was enhanced in RB tissues and cell lines.

Silencing of ZFPM2-AS1 Inhibits the Activity of RB Cells

We then examined whether the downregulation of ZFPM2-AS1 could affect the activity of RB cells. Silencing of ZFPM2-AS1 in Y79 and WERI-1 cells was found to hamper cell growth and promote apoptosis, but ZFPM2-AS1 restoration in RB cells contributed to promoted cell growth and inhibited apoptosis rate (Figs. 2A, 2B). After that, RT-quantitative PCR and immunofluorescence staining were applied to detect the expression of EMT-related proteins E-cadherin and N-cadherin in cells. Silencing of ZFPM2-AS1 increased E-cadherin expression, whereas inhibiting N-cadherin expression in cells, but overexpression of ZFPM2-AS1 in cells showed the opposite experimental results (Figs. 2C, 2D). Cell metastatic capacities were followingly investigated through transwell experiments, which revealed that the number of migrating and invading Y79 and WERI-1 cells was significantly reduced by ZFPM2-AS1 knockdown, but overexpression of ZFPM2-AS1 increased cell migration and invasion (Figs. 2E, 2F). To sum up, these results illustrated that ZFPM2-AS1 could contribute to the cell behaviors of RB cells.

ZFPM2-AS1 Sponges MiR-515 to Promote HOXA1 Expression

Using the LncAtlas (http://lncatlas.crg.eu/) database, the subcellular localization of ZFPM2-AS1 was predicted. We found that ZFPM2-AS1 was mainly localized in the cytoplasm (Fig. 3A). The results of cytoplasm/nucleus fractionation assay similarly demonstrated that ZFPM2-AS1 was mainly localized in the cytoplasm in Y79 and WERI-RB1 cells (Fig. 3B). Then, we used FISH experiments to detect localization in Y79 and WERI-1 cells. We found that red fluorescence was mainly distributed in the cytoplasm (Fig. 3C). The above experimental results suggested that ZFPM2-AS1 may regulate RB growth and metastasis through the ceRNA mechanism. Through the StarBase, miRDIP, and RNA22 databases, miRNAs containing binding sites with ZFPM2-AS1 were screened out, among which miR-515 was confirmed as a putative target of ZFPM2-AS1 by a luciferase reporter assay (Fig. 3D). We next detected the expression of miR-515 by RT-quantitative PCR and found that miR-515 expression was decreased significantly in RB cells (Fig. 3E). Moreover, overexpression or silencing of ZFPM2-AS1 negatively regulated the expression of miR-515 in Y79 and WRI-RB1

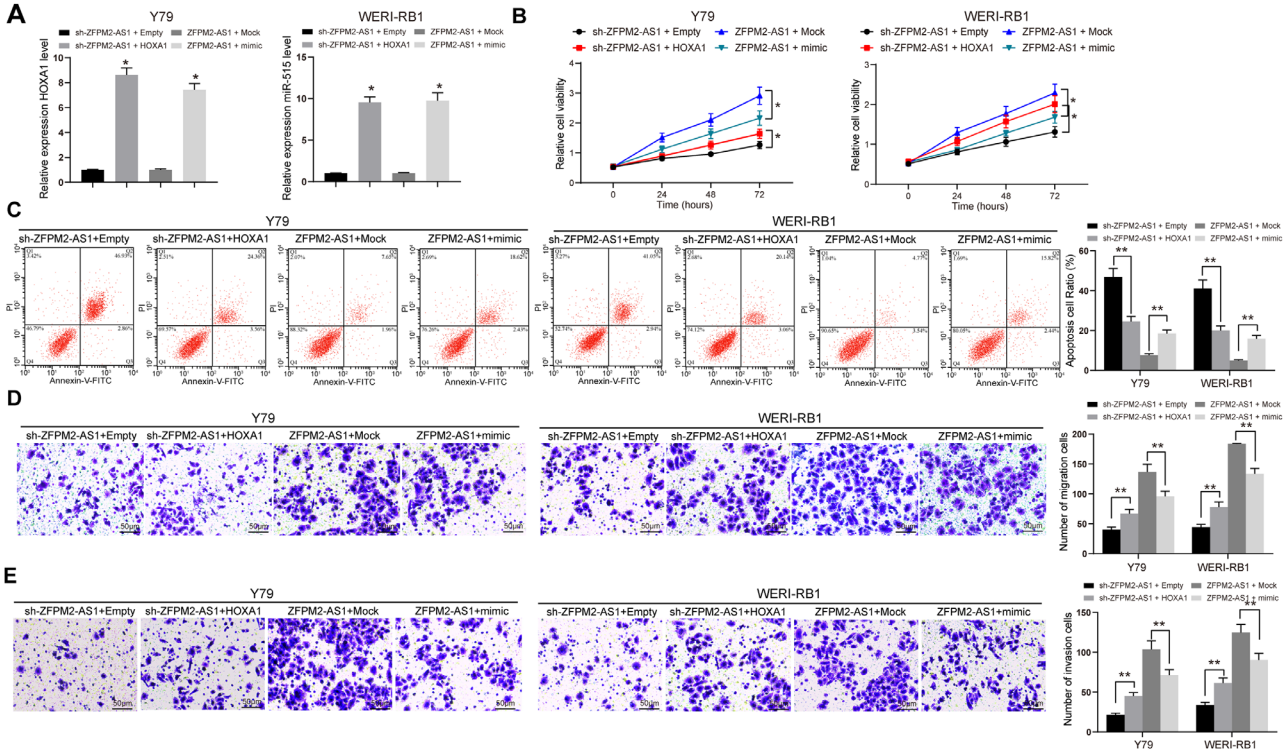

Figure 4. MiR-515 inhibits RB cell viability. (**A**) RT-quantitative PCR analysis of miR-515 expression pattern in Y79 and WERI-RB1 cells. (**B**) Cell viability determined by MTT assays. (**C**) PI/Annexin-V-stained cells determined by flow cytometric analysis. (**D**) Y79 and WERI-RB1 cell migration determined by transwell assays. (**E**) Y79 and WERI-RB1 cell invasion determined by transwell assays. The data are expressed as the mean ± SD. One-way ANOVA and Tukey's multiple comparison test was used to determine statistical significance, $^{*}P < 0.05$, $^{**}P < 0.01$.

cells (Fig. 3F). The similar converse regulation correlation between ZFPM2-AS1 and miR-515 was also validated in the collected clinical samples (Fig. 3G).

In order to further determine the downstream regulatory mechanism for miR-515, HOXA1, a target of miR-515 was predicted using miRSearch, TargetScan, and Miranda bioinformatics website prediction and confirmed using dual-luciferase reporter gene assays (Fig. 3H). In addition, HOXA1 also shared a positive correlation with ZFPM2-AS1 expression in 51 RB tissues (Figs. 3I, 3J). Taken together, ZFPM2-AS1 interacted with miR-515 to promote HOXA1 expression.

MiR-515 Overexpression Inhibits the Activity of RB Cells

Thus, Y79 and WERI-RB1 cells were co-transfected with sh-ZFPM2-AS1 + HOXA1 or ZFPM2-AS1 + miR-515 mimic, and RT-quantitative PCR verified the successful transfection (Fig. 4A). Subsequently, we found that after HOXA1 was overexpressed, the cell activity was partially restored, whereas after transfection of miR-515 mimic, the cell activity was significantly inhibited (Figs. 4B–E). To conclude, ZFPM2-AS1 played an oncogenic role in RB via miR-515/HOXA1 axis.

Silencing of ZFPM2-AS1 Blocks the Wnt/β-Catenin Signaling Pathway

The Wnt/β-catenin pathway signaling pathway is an extensively investigated pathway in RB.[18,19] Afterward, the expression of Wnt/β-catenin pathway-associated proteins in Y79 and WERI-RB1 cells was measured by ELISA and Western blot. After ZFPM2-AS1 knockdown, the expression of Wnt1 and β-catenin in Y79 and WERI-RB1 cells decreased, but the expression was partially restored after further overexpression of HOXA1. Although overexpression of ZFPM2-AS1 enhanced the expression of Wnt1 and β-catenin in Y79 and WERI-RB1 cells, the expression was inhibited after further transfection of miR-515 mimic (Figs. 5A, 5B). Moreover, we added Wnt/β-catenin pathway inhibitors C59 and RPI-724 in WERI-RB1 cells overexpressing ZFPM2-AS1, and observed that the cellular activity of cells was significantly inhibited (Figs. 5C–F). In summary, ZFPM2-AS1 potentiated the Wnt/β-catenin pathway activity to promote the RB progression.

ZFPM2-AS1 Knockdown Represses the Growth and Metastasis of RB In Vivo

To further verify the functional role of ZFPM2-AS1 on the growth of RB, we performed nude mouse tumorigenesis experiments. The downregulation of ZFPM2-AS1 in the Y79 cells inhibited RB growth rate in vivo (Figs. 6A, 6B) and the rate of KI67 positive cells (Fig. 6C) in the tumor. At last, through in vivo metastatic experiments, we found that ZFPM2-AS1 knockdown inhibited Y79 cell metastasis in vivo, showing a significant decline in the number of liver and lung metastatic nodules (Figs. 6D, 6E). Collectively, these findings implied that loss of function of ZFPM2-AS1

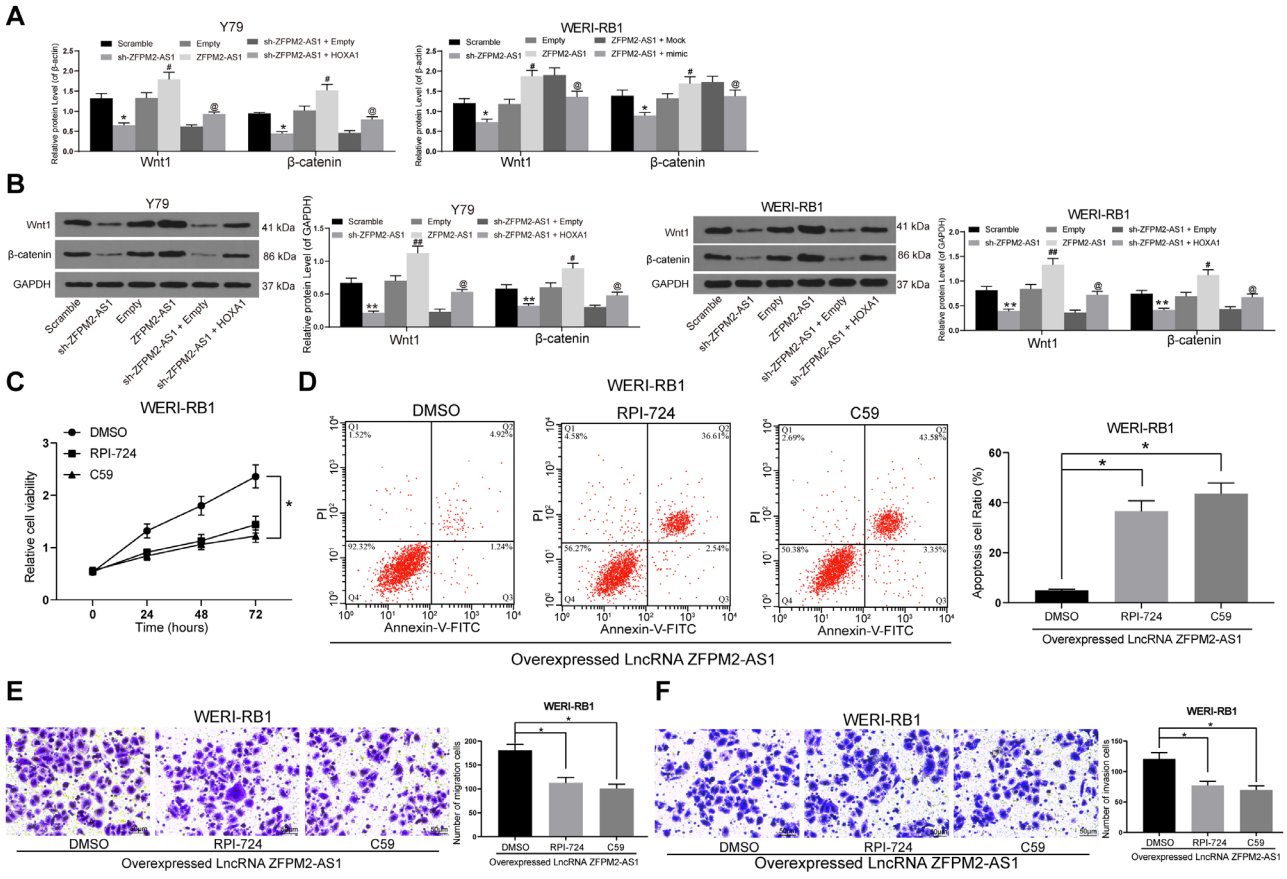

Figure 5. Wnt/β-catenin is prohibited when ZFPM2-AS1 is silenced. (**A**) Protein expression of Wnt1 and β-catenin in Y79 and WERI-RB1 cells determined by ELISA. (**B**) Protein expression of Wnt1 and β-catenin in Y79 and WERI-RB1 cells determined by Western blot. (**C**) Y79 and WERI-RB1 cell viability determined by MTT assays. (**D**) PI/Annexin-V-stained Y79 and WERI-RB1 cells determined by flow cytometry. (**E**) Y79 and WERI-RB1 cell migration determined by transwell assays. (**F**) Y79 and WERI-RB1 cell invasion determined by transwell assays. The data are expressed as the mean ± SD. One-way ANOVA and Tukey's multiple comparison test was used to determine statistical significance, $^{*}P < 0.05$, $^{**}P < 0.01$ vs. the Scramble or DMSO treatment; $^{\#}P < 0.05$, $^{\#\#}P < 0.01$ vs. empty treatment; $@P < 0.05$ vs. the ZFPM2-AS1 + mock treatment.

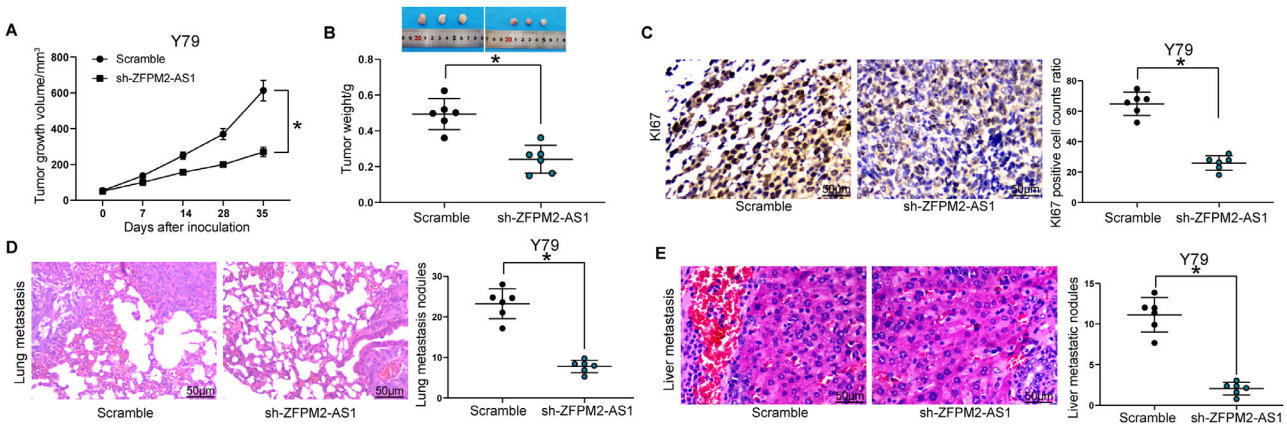

Figure 6. ZFPM2-AS1 knockdown prevents Y79 cells from growth and metastasis in vivo. (**A**) Xenograft tumor growth curve. (**B**) Xenograft tumor weight. (**C**) KI67 positive cell ratio in Y79 cells determined by immunohistochemistry. (**D**) Lung metastasis determined by hematoxylin eosin (HE) staining. (**E**) Liver metastasis determined by HE staining. The data are expressed as the mean ± SD. One-way ANOVA and Tukey's multiple comparison test was used to determine statistical significance, $^{*}P < 0.05$.

Investigative Ophthalmology & Visual Science

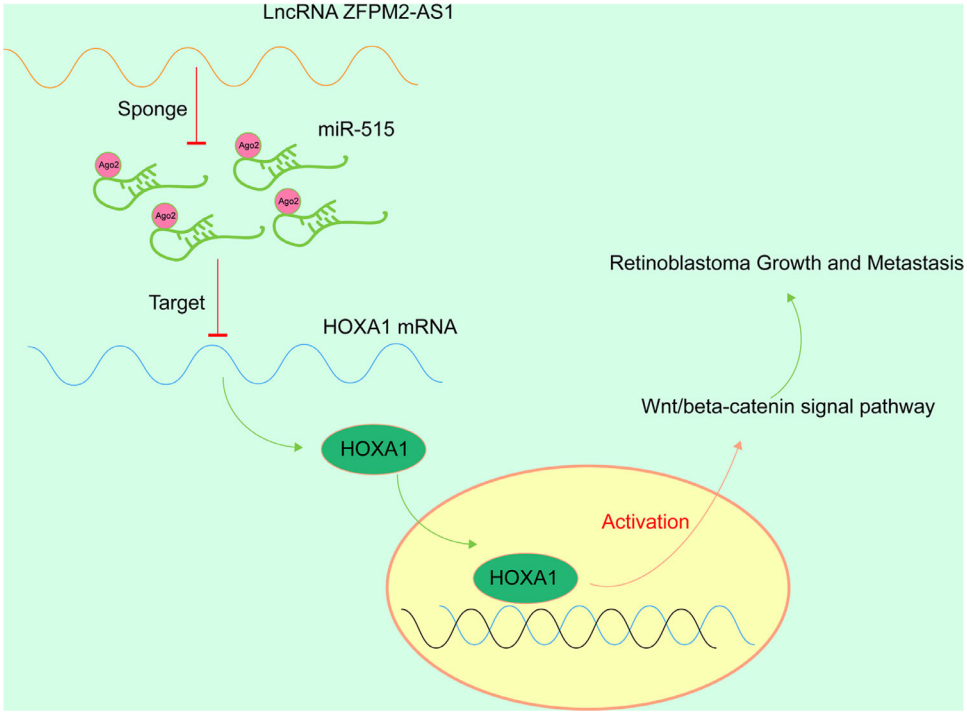

Figure 7. Schematic of the topic. ZFPM2-AS1 promotes the growth and metastasis of RB by sponging miR-515 to target HOXA1 via the Wnt/β-catenin signaling pathway.

suppressed tumor xenograft growth and metastasis of Y79 cells in vivo.

Discussion

RB contributes to 3% of pediatric cancers among the children population under 15 years of age, and intra-arterial and fluoroscopy-guided chemotherapy is utilized for cases of advanced RB grades higher than B.[20] Because RB tends to metastasize, the visual function and the life health of patients are under great risks.[18] In the present report, we revealed that ZFPM2-AS1 was upregulated in RB tissue samples and cells. Overexpression of ZFPM2-AS1 promoted the viability, migration, and invasion capacities of WERI-RB1 cells. Suppression of ZFPM2-AS1 had reverse effects in Y79 cells in vitro as well as in vivo. Moreover, ZFPM2-AS1 negatively regulated the expression of miR-515 in Y79 and WERI-RB1 cells. MiR-515 played as a tumor inhibitor in RB cells by inhibiting cell viability, migration, and invasion, yet accelerating apoptosis. Furthermore, ZFPM2-AS1 positively regulated HOXA1 expression, which was a putative target of miR-515 in RB cells via the Wnt/β-catenin signaling pathway.

Previous evidence has proved that ZFPM2-AS1 promoted renal cell cancer cell metastasis and proliferation, while repressing its apoptosis.[21] Our study showed that ZFPM2-AS1 was enhanced in RB samples and cells and correlated with worse prognosis of patients. Besides, following restoration of ZFPM2-AS1, the growth and EMT of RB cells were promoted by upregulating N-cadherin and downregulating E-cadherin. The above findings specified that ZFPM2-AS1 potentiated tumorigenesis of RB, which might perform as an oncogene. We sought to clarify the molecular mechanisms where ZFPM2-AS1 enhanced proliferation and metastasis in RB. The ceRNAs are RNA transcripts that communicate with each other by decreasing targeting miRNA expression with the derepression of other mRNAs having the common miRNA response elements.[22] Dysfunction of ceRNA and ceRNA networks may result in different kinds of diseases, but, on the other hand, it may be used to elucidate disease processes and provide new opportunities for treatment.[23] Through StarBase, miRDIP, and RNA22 databases, we predicted miR-515 as a target of ZFPM2-AS1. Furthermore, ZFPM2-AS1 expression in RB tissues and cell lines conversely correlated with miR-515 level, and miR-515 overexpression could partly reverse the promotive effects on RB cell growth, migration, and invasion induced by ZFPM2-AS1 overexpression. In line with our results, Pardo et al. reported that miR-515-5p expression was inversely linked to metastasis in mice with breast and lung cancers.[24] These findings indicated that ZFPM2-AS1 might exert its tumor-initiating activity through binding to miR-515.

To further explore how miR-515 regulates the malignant aggressiveness in RB, we performed bioinformatics analysis and dual-luciferase reporter gene experiments that identified HOXA1 as a candidate mRNA for miR-515. Similarly, miR-515-5p was found to be sponged by LINC00673 to downregulate MARK4 expression, thereby disrupting the Hippo pathway in breast cancer.[25] Likewise, lung adenocarcinoma cell proliferation was weakened by ZFPM2-AS1 depletion, but this trend was partly reversed by overexpression of VMA21, a target of miR-18b-5p.[26] Interestingly, we also observed that knockdown of ZFPM2-AS1 lowered the expression of Wnt1 and β-catenin expression in Y79 cells, whereas resumption of HOXA1 led to a partial upregulation. β-catenin, implicated in abundant interactions between proteins, is believed to be the essential hub of the Wnt pathway.[27] In line with our outcomes, the expression of β-catenin was remarkably elevated in WERI-RB1 cells overexpressing MEG3 and dimin-

ished in Y79 cells harboring MEG3 knockdown versus the control treatments, respectively.[28] Moreover, the significance of the Wnt/β-catenin signaling pathway in sustaining the phenotype of epithelial cell, cell junctions in addition to tissue homeostasis have been underscored previously.[29] As a consequence, the Wnt/β-catenin inhibitors C59 and RPI-724 contributed to significant declines in cell growth, migration, and invasion, whereas promotions in cell apoptosis of WERI-RB1 cells overexpressing ZFPM2-AS1.

A potential limitation of the current report is that we only corroborated the correlation between miR-515 and HOXA1, it is undefined that HOXA1 has the stimulative effects on RB progression and metastasis. Besides, although Wnt/β-catenin inhibitors hamper the malignancy phenotypes of WERI-RB1 cells, which was verified in the present study, a mouse model might be more supporting. Furthermore, ZFPM2-AS1 was reported to facilitate gastric carcinogenesis by attenuating the p53 pathway.[8] Indeed, we cannot exclude the involvement of the p53 pathway in the development of RB. However, due to the time and funding limitations, whether this was another survival mechanism for RB was not probed in the current study, which might be the direction of further investigations. In summary, our study showed that ZFPM2-AS1 functioned as an oncogene in RB cells by suppressing the tumor suppressor miR-515, thereby promoting cell growth, migration, invasion in vitro, and xenograft growth and metastasis in nude mice (Fig. 7). In addition, the effects of ZFPM2-AS1 on cell viability, invasion, and migration in vitro could be abolished by miR-515 mimic or restoring HOXA1 expression, during which the Wnt/β-catenin pathway was involved. This new axis may be introduced as a possible indicator to detect RB, eliciting beneficial therapeutic effects for this malignancy.

Acknowledgments

Supported by the Jilin Province Education Department 135 Project (Grant No. JJKH20170810KJ).

Disclosure: **X. Lyv**, None; **F. Wu**, None; **H. Zhang**, None; **J. Lu**, None; **L. Wang**, None; **Y. Ma**, None

References

1. Zhang J, Benavente CA, McEvoy J, et al. A novel retinoblastoma therapy from genomic and epigenetic analyses. *Nature*. 2012;481:329–334.
2. Abramson DH, Shields CL, Munier FL, Chantada GL. Treatment of retinoblastoma in 2015: agreement and disagreement. *JAMA Ophthalmol*. 2015;133:1341–1347.
3. Gunduz K, Muftuoglu O, Gunalp I, Unal E, Tacyildiz N. Metastatic retinoblastoma clinical features, treatment, and prognosis. *Ophthalmology*. 2006;113:1558–1566.
4. Yang L, Zhang L, Lu L, Wang Y. Long noncoding RNA SNHG16 sponges miR-182-5p and miR-128-3p to promote retinoblastoma cell migration and invasion by targeting LASP1. *Onco Targets Ther*. 2019;12:8653–8662.
5. Bhan A, Soleimani M, Mandal SS. Long noncoding RNA and cancer: a new paradigm. *Cancer Res*. 2017;77:3965–3981.
6. Yang G, Fu Y, Lu X, Wang M, Dong H, Li Q. LncRNA HOTAIR/miR-613/c-met axis modulated epithelial-mesenchymal transition of retinoblastoma cells. *J Cell Mol Med*. 2018;22:5083–5096.
7. Cheng Y, Chang Q, Zheng B, Xu J, Li H, Wang R. LncRNA XIST promotes the epithelial to mesenchymal transition of retinoblastoma via sponging miR-101. *Eur J Pharmacol*. 2019;843:210–216.
8. Kong F, Deng X, Kong X, et al. ZFPM2-AS1, a novel lncRNA, attenuates the p53 pathway and promotes gastric carcinogenesis by stabilizing MIF. *Oncogene*. 2018;37:5982–5996.
9. Li J, Ge J, Yang Y, Liu B, Zheng M, Shi R. Long noncoding RNA ZFPM2-AS1 is involved in lung adenocarcinoma via miR-511-3p/AFF4 pathway. *J Cell Biochem*. 2020;121:2534–2542.
10. Li J, Tang Z, Wang H, et al. CXCL6 promotes non-small cell lung cancer cell survival and metastasis via down-regulation of miR-515-5p. *Biomed Pharmacother*. 2018;97:1182–1188.
11. Wardwell-Ozgo J, Dogruluk T, Gifford A, et al. HOXA1 drives melanoma tumor growth and metastasis and elicits an invasion gene expression signature that prognosticates clinical outcome. *Oncogene*. 2014;33:1017–1026.
12. Wang H, Liu G, Shen D, et al. HOXA1 enhances the cell proliferation, invasion and metastasis of prostate cancer cells. *Oncol Rep*. 2015;34:1203–1210.
13. Xu H, Zhao H, Yu J. HOXB5 promotes retinoblastoma cell migration and invasion via ERK1/2 pathway-mediated MMPs production. *Am J Transl Res*. 2018;10:1703–1712.
14. Zhang Y, Fang J, Zhao H, Yu Y, Cao X, Zhang B. Downregulation of microRNA-1469 promotes the development of breast cancer via targeting HOXA1 and activating PTEN/PI3K/AKT and Wnt/beta-catenin pathways. *J Cell Biochem*. 2019;120:5097–5107.
15. Silva AK, Yi H, Hayes SH, Seigel GM, Hackam AS. Lithium chloride regulates the proliferation of stem-like cells in retinoblastoma cell lines: a potential role for the canonical Wnt signaling pathway. *Mol Vis*. 2010;16:36–45.
16. Hu WY, Wei HY, Li KM, Wang RB, Xu XQ, Feng R. LINC00511 as a ceRNA promotes cell malignant behaviors and correlates with prognosis of hepatocellular carcinoma patients by modulating miR-195/EYA1 axis. *Biomed Pharmacother*. 2020;121:109642.
17. Wan W, Wan W, Long Y, et al. MiR-25-3p promotes malignant phenotypes of retinoblastoma by regulating PTEN/Akt pathway. *Biomed Pharmacother*. 2019;118:109111.
18. Yu F, Pang G, Zhao G. ANRIL acts as onco-lncRNA by regulation of microRNA-24/c-Myc, MEK/ERK and Wnt/beta-catenin pathway in retinoblastoma. *Int J Biol Macromol*. 2019;128:583–592.
19. Liao YJ, Yin XL, Deng Y, Peng XW. PRC1 gene silencing inhibits proliferation, invasion, and angiogenesis of retinoblastoma cells through the inhibition of the Wnt/beta-catenin signaling pathway. *J Cell Biochem*. 2019;120:16840–16852.
20. Obesso A, Alejo L, Huerga C, et al. Eye lens radiation exposure in paediatric interventional treatment of retinoblastoma. *Sci Rep*. 2019;9:20113.
21. Liu JG, Wang HB, Wan G, Yang MZ, Jiang XJ, Yang JY. Long noncoding RNA ZFPM2-AS1 promotes the tumorigenesis of renal cell cancer via targeting miR-137. *Eur Rev Med Pharmacol Sci*. 2019;23:5675–5681.
22. Ergun S, Oztuzcu S. Oncocers: ceRNA-mediated cross-talk by sponging miRNAs in oncogenic pathways. *Tumour Biol*. 2015;36:3129–3136.
23. Salmena L, Poliseno L, Tay Y, Kats L, Pandolfi PP. A ceRNA hypothesis: the Rosetta Stone of a hidden RNA language? *Cell*. 2011;146:353–358.
24. Pardo OE, Castellano L, Munro CE, et al. miR-515-5p controls cancer cell migration through MARK4 regulation. *EMBO Rep*. 2016;17:570–584.
25. Qiao K, Ning S, Wan L, et al. LINC00673 is activated by YY1 and promotes the proliferation of breast cancer cells

Investigative Ophthalmology & Visual Science

via the miR-515-5p/MARK4/Hippo signaling pathway. *J Exp Clin Cancer Res*. 2019;38:418.

26. Xue M, Tao W, Yu S, et al. lncRNA ZFPM2-AS1 promotes proliferation via miR-18b-5p/VMA21 axis in lung adenocarcinoma. *J Cell Biochem*. 2020;121:313–321.
27. Xiao W, Chen X, He M. Inhibition of the Jagged/Notch pathway inhibits retinoblastoma cell proliferation via suppressing the PI3K/Akt, Src, p38MAPK and Wnt/betacatenin signaling pathways. *Mol Med Rep*. 2014;10:453–458.
28. Gao Y, Lu X. Decreased expression of MEG3 contributes to retinoblastoma progression and affects retinoblastoma cell growth by regulating the activity of Wnt/beta-catenin pathway. *Tumour Biol*. 2016;37:1461–1469.
29. Wang BM, Li N. Effect of the Wnt/beta-catenin signaling pathway on apoptosis, migration, and invasion of transplanted hepatocellular carcinoma cells after transcatheter arterial chemoembolization in rats. *J Cell Biochem*. 2018;119:4050–4060.

Investigative Ophthalmology & Visual Science